

## A study of electron excitations in $\text{CaWO}_4$ and $\text{PbWO}_4$ single crystals

This article has been downloaded from IOPscience. Please scroll down to see the full text article.

1997 J. Phys.: Condens. Matter 9 249

(<http://iopscience.iop.org/0953-8984/9/1/026>)

View [the table of contents for this issue](#), or go to the [journal homepage](#) for more

Download details:

IP Address: 171.66.16.207

The article was downloaded on 14/05/2010 at 06:04

Please note that [terms and conditions apply](#).

## A study of electron excitations in $\text{CaWO}_4$ and $\text{PbWO}_4$ single crystals

V Mürk†, M Nikl‡, E Mihoková‡ and K Nitsch‡

† Institute of Physics, Riia 142, EE2400 Tartu, Estonia

‡ Institute of Physics, Academy of Sciences of the Czech Republic, Cukrovarnická 10, 162 00 Prague, Czech Republic

Received 2 July 1996, in final form 10 September 1996

**Abstract.** The excitation spectra of photo- and thermo-luminescence were compared in the VUV–UV spectral region in  $\text{CaWO}_4$  and  $\text{PbWO}_4$  scheelite tungstates. Temperature dependences of emission intensities and decay times were measured for  $\text{PbWO}_4$  in the 80–300 K range and approximated by a simple phenomenological model. The energy level structure of the emission centre excited state and related kinetic processes are discussed for both tungstates.

### 1. Introduction

Photoluminescence (PL) of Ca and Pb scheelite tungstates has been already studied by several authors [1–4]. Two emission components were identified in the emission spectra in both crystals, namely, a blue one peaking at 420–440 nm and ascribed to the  $(\text{WO})_4$  complex anion centre and another one peaking in the green–yellow spectral region. The latter component exhibits different positions in  $\text{PbWO}_4$  (PWO) and  $\text{CaWO}_4$  (CWO) crystals and usually is ascribed to the  $\text{WO}_3$  defect centre. The strong difference, e.g., in excitation spectra of the two components in PWO and CWO at low temperatures [1, 2, 5] supports the important role of  $\text{Pb}^{2+}$  ions, particularly in non-relaxed excited states of the emission centres.

The thermostimulated luminescence (TSL) spectra of CWO [6] and PWO [7, 8] under x-ray excitation show several peaks below and also above room temperature (RT), which gives evidence of the variety of trap states present in these materials.

The PL decay kinetics of CWO [2] and PWO [3, 5] shows a strong decrease of the decay times with increasing temperature. Slower non-exponential components were noticed in PWO PL decay above 180 K and ascribed to the radiative recombination of free carriers created even under selective sub-gap excitation at  $\lambda_{exc} > 310$  nm [5]. While in CWO the emission intensity is weakly temperature dependent below 300 K, in PWO a strong decrease in both spectral components was reported in steady-state x-ray excited luminescence above 200 K [5]. There has been no reported attempt to evaluate simultaneously the temperature dependences of decay times and intensities in PWO to compare the emission properties of PWO and CWO. Such an attempt is highly desirable because of the rather complicated character of PWO emission.

It is the aim of this paper to compare the relaxation processes and excited state dynamics in PWO and CWO and to model the above-mentioned temperature dependences of PWO emission characteristics within a simple phenomenological approach.

## 2. Experimental details

The luminescence spectra in the VUV–UV–visible region have been measured using hydrogen/deuterium discharge lamp excitation and corrected for instrumental characteristics (for details see [9] and [10]). Thermoluminescence (TL) spectra were measured in the regime of linear storage to exclude the influence of the trap saturation effects. In the decay kinetics measurements, pulsed x-ray and hydrogen filled flashlamps were used as the excitation sources and the single-photon counting method was applied for the detection. By means of a deconvolution procedure the true decay times were extracted from the decay curves measured.

Polished samples have been prepared from single-crystal boules grown by the Czochralski method having size about  $7 \times 7 \times 1 \text{ mm}^3$ . PWO sample No 1 (PWO1) was grown from 5N raw material [11]. PWO sample No 2 was grown from 4N raw material doped with about 30 ppm of  $\text{Nb}^{5+}$  in the crystal [12]. These PWO samples were selected to exhibit considerably different absolute intensity of the green component. In the steady-state x-ray excited emission spectra [11], this component is almost absent from PWO1, while it prevails in PWO2 (PWO894 in [11]). The CWO crystal was grown in the State Optical Institute, St Petersburg, Russia.

## 3. Experimental results and discussion

At 80 K, excitation spectra of the blue emission components show sharp edges at 4.8 and 4.0 eV in CWO and PWO, respectively (figure 1). These edges tend to move to the long-wavelength side with increasing temperature. In contrast, the excitation peaks of the low-energy emission components (figure 1) are rather weakly temperature dependent and consist mainly of the peak at the long-wavelength side of the blue component excitation edge mentioned. The absolute height of these peaks in PWO depends strongly on a particular crystal and is correlated with the intensity of the very slow processes in the luminescence decay [5] and the integrated intensity of the TSL signal over the 220–300 K range [13]. The behaviour of the blue-component excitation spectra is characteristic for the excitation within the intrinsic Urbach absorption edge, where with elevating temperature the intrinsic absorption overlaps the closely lying absorption bands of defect centres and suppresses their excitation, as clearly observed for CWO. In PWO analogous suppression is probably efficient above 250 K, but it is obscured because of simultaneous thermal quenching of both the blue and green emission components. Strong short-wavelength decrease of excitation efficiency (connected evidently with the surface losses, as shown for  $\text{PbMoO}_4$  in [14]) starts in the vicinity (about 1 eV) of the PWO intrinsic transition edge, whereas it occurs at a distance of more than 2 eV from the CWO respective edge (figure 1 and [15]).

TSL glow curves of PWO and CWO measured in the temperature interval 80–240 K are represented in figure 2. In the case of PWO, the TSL peaks are observed at about 110 and 190 K in agreement with [8] and [13]; for CWO, the peak at 160 K has been reported as well [6].

The temperature dependences of selectively UV excited decay times of the blue- and green-PWO-emission components are given in figure 3. Non-selective excitation by a pulsed x-ray source gives essentially the same decay times. In the case of a few nanosecond broad x-ray pulses the amplitude of the emission pulse remains the same in the whole temperature interval of quenching, implying a temperature-independent initial population of the emitting states. In the consequence, the main part of PWO fast emission at room temperature represents the rest of the strongly quenched ‘blue’ emission. Additional slower

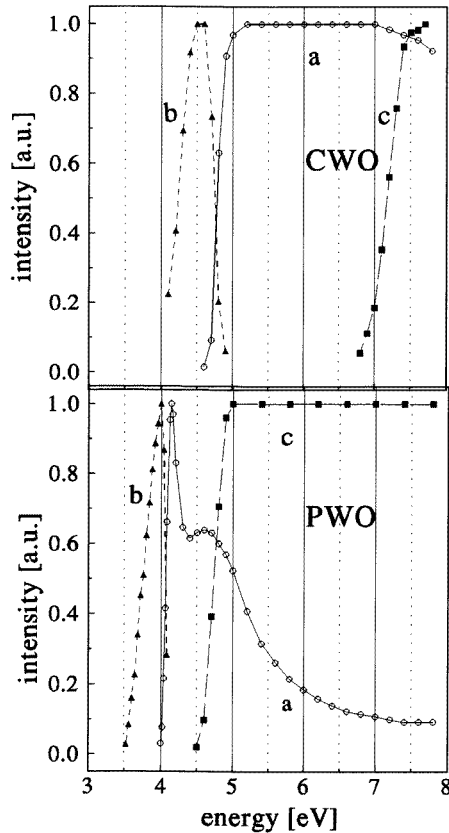


**Figure 1.** Excitation spectra are given separately for CWO and PWO,  $T = 80$  K: (a) the excitation spectrum of the blue emission component,  $\lambda_{em} = 400$  nm; (b) the excitation spectrum of the green–yellow emission component,  $\lambda_{em} = 520$  nm; (c) the excitation spectrum of TL (peaks at 110 and 160 K for PWO and CWO, respectively).

components are sample dependent [5], which is also observed here comparing two PWO samples measured, and this reflects the defect-induced processes. With respect to UV excitation, the presence of slower components, mainly in the green emission component, is enhanced, which is observed also for 511 keV photon excitation by the  $\text{Na}^{22}$  radioisotope [5].

Below the onset of thermal quenching, when the total yield of the blue-emission component does not change, the manifestations of at least a two-level structure of emitting centre responsible for the changes of decay time are observable in both kinds of tungstate. This is characteristic mainly in the case of CWO, where the emission intensity is only about halved at 300 K with respect to 4 K, while the related decay time is shortened by more than an order of magnitude [2]. Consequently, it can be deduced that the main difference between two tungstates discussed seems to be connected with the different quenching temperature—the emission intensity decreases to 50% of its 80 K value at about 300 and 160 K in the Ca and Pb tungstates, respectively.

To measure the temperature dependences (TDs) of PWO emission, a bandlike excitation within 280–350 nm was used to avoid additional changes of the initial excitation population

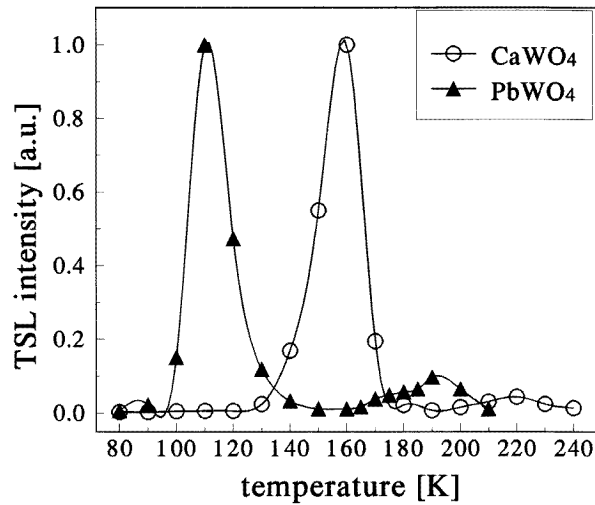


Figure 2. TL glow curves of PWO2 and CWO crystals after x-ray irradiation at  $T = 80$  K.

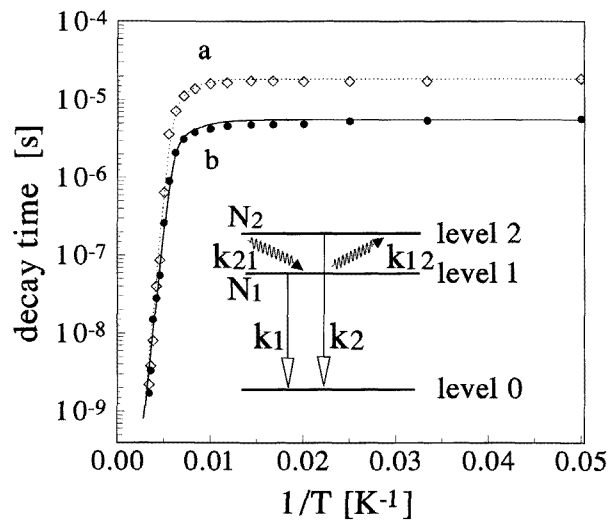
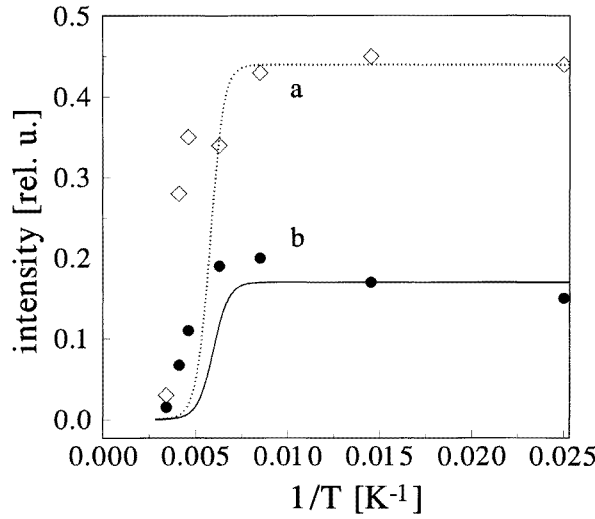


Figure 3. Temperature dependences of the blue- and green-component decay times,  $\lambda_{em} = 400$  and 520 nm, respectively. The excitation wavelength was chosen in the maximum of the excitation spectrum at each temperature, i.e., in the interval 295–310 nm and close to 310 nm for the blue and green components, respectively. The lines are determined from the model calculations described in the text. The inset shows a sketch of the excited level arrangement for the blue- and green-emission centres in PWO and related parameters for the model described in the text.

because of the temperature dependent position and halfwidth of the related excitation peak of the blue component. From the emission spectra obtained, the blue and green components were separated using a four-Gaussian decomposition of the spectra (for details see [5]). The results are given in figure 4.



**Figure 4.** The TDs of the blue- and green-component-emission intensities of PWO under bandlike excitation, 280–350 nm (for details of the evaluation see [5]). The lines follow from the model calculations described in the text.

To determine better the relation between the TD of the decay times and emission intensities in PWO, a simple three-level model was adopted (inset in figure 3). It is similar to that used, e.g., for  $\text{Pb}^{2+}$  centre emission in  $\text{Cs}_4\text{PbCl}_6$  [16], because the characteristics of the levels responsible for the radiative transition are probably similar in  $\text{Cs}_4\text{PbCl}_6$  and  $\text{PbWO}_4$  ( $^3\text{T}_1$  and  $^1\text{A}_1$  are the terms describing the lowest excited and the ground states, respectively). In the inset in figure 3,  $N_1$  and  $N_2$  are the occupations of the levels 1 and 2,  $k_1$  and  $k_2$  the radiative transition rates and  $k_{12}$  and  $k_{21}$  the nonradiative transition rates between the levels 1 and 2 taken as a one-phonon process, i.e.,

$$\begin{aligned} k_{21} &= K(n_B + 1) \\ k_{12} &= Kn_B \end{aligned} \quad (1)$$

where  $K$  is the transition rate at  $T = 0$  K and

$$n_B = 1/\exp[D/k_B T - 1] \quad (2)$$

is the Bose–Einstein distribution of phonons with  $D$  being the energy separation between the levels 1 and 2. The time evolution of the level occupations  $N_{1,2}$  can be described by the rate equation in a matrix form

$$\frac{d}{dt} \begin{pmatrix} N_1 \\ N_2 \end{pmatrix} = \begin{pmatrix} -(k_1 + k_{12}) & k_{21} \\ k_{12} & -(k_2 + k_{21}) \end{pmatrix} \begin{pmatrix} N_1 \\ N_2 \end{pmatrix}. \quad (3)$$

The analytical solution of (3) is given in the form

$$N_i(t) = \sum_i A_i \exp[-t/\tau_i] \quad i = 1, 2. \quad (4)$$

Two inverse decay times  $\tau_i$  are given by eigenvalues of the matrix of the coefficients in (3) and the total luminescence intensity released can be expressed as follows:

$$I = \int_0^\infty \sum_i (k_i N_i) dt \quad i = 1, 2. \quad (5)$$

The single-exponential character of the decay observed at the lowest temperature in both spectral components of PWO emission can be explained by the assumption  $N_2(t = 0) = 0$ . In the low-temperature limit  $T \rightarrow 0$ , the inverse non-radiative transition parameter can be neglected and one can find  $k_1$  using the decay time  $\tau_1$  measured,

$$k_1 = 1/\tau_1. \quad (6)$$

The rest of the parameters, namely  $k_2$ ,  $K$  and  $D$  can be determined from the best fit of the experimental temperature dependence of the decay times in figure 3. Nonradiative quenching to the ground state is considered from level 1 in the classical exponential form of the quenching rate  $k_x = K_x \exp[-E_x/kT]$ .

The best-fit parameters for the approximations in figure 3 (decay times) are collected in table 1 and were used to fit the TD of emission intensities in figure 4. Clear disagreement above 170 K is demonstrated, which cannot be improved by any variation of parameters while keeping agreement with the decay time data in figure 3. Essentially the same results are obtained for the UV bandlike excitation 250–350 nm or x-ray excitation of steady-state emission spectra (the experimental data of the latter are given in [5]). Such a disagreement can be explained, e.g., by thermally induced disintegration of the photo-excited states producing free electrons and holes. These free carriers can experience radiative recombination at (the same) emission centres at a later stage. Such a process (considered in the relaxed excited state) leads to the shortening of the decay times observed, while keeping (steady-state) emission intensity unchanged. As a limit case one could consider the activation energy of quenching  $E_x = 230$  (270) meV given in table 1 for the blue- (green-) emission component as the thermoionization energy of the related emission centre excited state and non-radiative quenching to the ground state might even be absent as in CWO at these temperatures.

**Table 1.**

Parameter	Blue component	Green component
$k_1$ (s <sup>-1</sup> )	$1.8 \times 10^5$	$5.4 \times 10^4$
$k_2$ (s <sup>-1</sup> )	$5 \times 10^6$	$5 \times 10^6$
$K$ (s <sup>-1</sup> )	$10^{10}$	$10^{10}$
$d$ (meV)	45	60
Parameter	Quenching from level 1	Quenching from level 1
$K_x$ (s <sup>-1</sup> )	$3 \times 10^{12}$	$10^{13}$
$E_x$ (meV)	230	270

To examine this hypothesis in detail, the TL excitation spectra of PWO were measured at elevated temperatures using the TSL peak at about 190 K. In figure 5, the distinct changes in TSL excitation spectrum can be seen, as compared with figure 1(c). Actually, at  $T > 150$  K TSL is efficiently excited at the same spectral region as both components in PL (their excitation spectra are given in figure 5 at 150 K as well). As a consequence, this result evidences increasing probability of thermally induced disintegration of the respective excited state at these temperatures. As shown by the comparison of PL and TL excitation spectra, such thermal disintegration at its initial stage is the most pronounced in the narrow energy region of the probable Pb exciton peak. Speaking in more detail, one can consider for the final state of disintegration the holes in the oxyanion states, which are mobile according to EPR studies [7], and the electron in the Pb<sup>+</sup> states. If the high-energy edge of TL

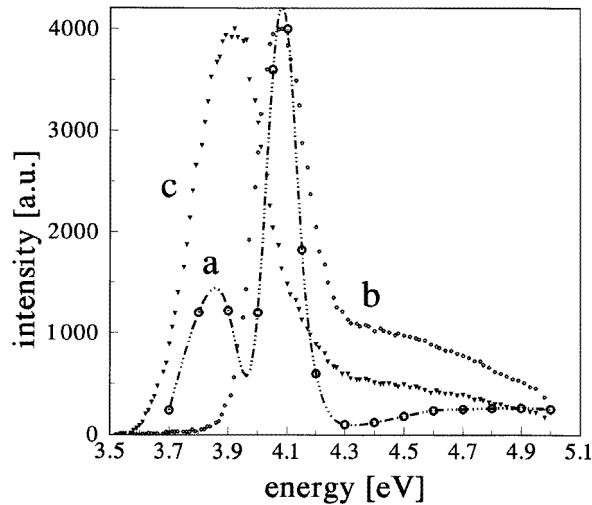


**Figure 5.** The excitation spectrum of PWO TL (190 K TSL peak) at 152 K (a) and excitation spectra of the blue- (b) and green- (c) PWO-emission components,  $\lambda_{em} = 400$  and 520 nm, respectively,  $T = 150$  K.

excitation in CWO is the edge of Ca-related states [15] (i.e., the hole in the oxyanion state and the electron in the  $\text{Ca}^+$  one), then (taking into account the second ionization potentials of Ca ( $-11.87$  eV) and Pb ( $-15.04$  eV) and also the fact that the Madelung potential must be approximately the same in both tungstates) we could estimate the energy of the state consisting of the tungstate group related hole and the electron in the  $\text{Pb}^+$  state. It should be about 3.2 eV lower than the TL excitation edge in CWO, i.e., about 4 eV, which is reasonably close to the experimental value of the PL excitation edge in PWO at 80 K—see figure 1. Although the direct observation of these, in fact, charge-transfer transitions seems to be less probable on the background of the strongly allowed  $s$ - $p$  transition in the  $\text{Pb}^{2+}$  ion, this electron-hole continuum may affect essentially the stability of excitons.

It is worth stressing that, according to this interpretation, free electron and holes are generated under any excitation wavelength in both PWO luminescence components above 150 K and there is always thermal equilibrium between exciton and free electron-hole states. Taking into account possibly slow diffusion of free carriers (further slowed down by presence of shallow traps [13]) followed by their radiative recombination at the blue- and green-emission centres, one can understand the presence of very slow-decay components observed in PWO luminescence and scintillation at room temperature [5, 13].

Another important feature is related to the long-wavelength edges of the TL excitation spectra—see figure 1. In contrast to the above-discussed thermoionization processes, they represent the true edges of band-to-band transitions, which are responsible for the temperature-independent charge separation. In the case of  $\text{CaWO}_4$  such an edge could be connected [15, 17] with the scattering between oxyanion excited states and the continuum of states involving an oxycomplex-related hole and the electron in the  $\text{Ca}^+$  state. A similar edge of the low-temperature TL excitation spectrum is observable in PWO crystals at 4.8 eV, coinciding with the edge of  $\text{CaWO}_4$  intrinsic transitions observed in the blue-component excitation spectrum, the latter belonging obviously to the transitions between oxyanion states. A remarkably different situation seems to be realized at the interaction of a molecular type exciton and the electron-hole continuum states in the Pb and Ca tungstates—in the



former case the lowest unrelaxed states are Pb-related ones, whereas in the latter case those belonging to the oxyanion group.

Thus, although a strong difference of both reflectivity [18] and the excitation edge of Pb tungstate from those of other tungstates shows the lowest intrinsic optical transitions are associated with the 6s–6p ones in the  $\text{Pb}^{2+}$  ion, the oxycomplex states play an important role in subsequent relaxation processes and radiative de-excitation in PWO as well.

#### 4. Conclusion

It follows from the comparison of PL and TL excitation spectra of PWO and CWO that  $\text{Pb}^{2+}$  ions determine the non-relaxed excited state characteristics in PWO. Furthermore, the description of temperature dependences of emission intensities and decay times in PWO by three-level model shows that it is impossible to explain the observed dependences only in terms of thermally induced transitions within two excited state levels and additional thermal quenching to the ground state. The evidence of thermally induced decomposition of the excited state in both the blue and green components in PWO above 150 K was obtained comparing PL and TL excitation spectra at elevated temperatures. Such a process can explain the observed discrepancy between the experimental temperature dependences of the decay times and emission intensities and the phenomenological model discussed. At sufficiently high temperatures the unavoidable participation of free carriers in the overall decay kinetics can explain the presence of very slow and non-exponential components observed in PL and scintillation decays above 180 K [5, 13], taking into account possibly slow diffusion of free carriers before their radiative recombination.

#### Acknowledgments

The authors are grateful to P Lecoq from CERN for providing us the PWO sample for the experiments and to K Polak for fruitful discussions. The partial financial support of the EC network grant ERBCIPDCT 940037 is also gratefully acknowledged.

#### References

- [1] Grasser R and Scharmann A 1976 *J. Lumin.* **12/13** 473
- [2] Treadaway M J and Powell R C 1974 *J. Chem. Phys.* **61** 4003
- [3] Van Loo W 1975 *Phys. Status Solidi a* **27** 565; **28** 227
- [4] Groenink J A and Blasse G 1980 *J. Solid State Chem.* **32** 9
- [5] Nikl M, Nitsch K, Polak K, Mihokova E, Dafinei I, Auffray E, Lecoq P, Reiche P, Uecker R and Pazzi G P 1996 *Phys. Status Solidi b* **195** 311
- [6] Hofstaetter A, Planz J and Scharmann A 1977 *Z. Naturf.* a **32** 957
- [7] Hofstaetter A, Oeder R, Scharmann A, Schwabe D and Vitt B 1978 *Phys. Status Solidi b* **89** 375
- [8] Auffray E, Dafinei I, Lecoq P and Schneegans M 1995 *Radiat. Eff. Defects Solids* **135** 343
- [9] Murk V V and Ismailov K M 1993 *Sov. Phys.–Solid State* **35** 259; 1992 *Sov. Phys.–Solid State* **34** 165
- [10] Polak K, Birch D J S and Nikl M 1988 *Phys. Status Solidi b* **145** 741
- [11] Nitsch K, Nikl M, Ganschow S, Reiche P and Uecker R 1996 *J. Crystal Growth* **165** 163
- [12] Lecoq P et al 1995 *Nucl. Instrum. Methods A* **365** 291
- [13] Martini M, Spinolo G, Vedda A, Nikl M, Nitsch K, Hamplova V, Fabeni P, Pazzi G P, Dafinei I and Lecoq P 1996 *Chem. Phys. Lett.* **260** 418
- [14] Reut E G 1981 *Opt. Spectrosc.* **50** 821 (in Russian)
- [15] Gurvich A M, Ilmas E R, Savihhina I T and Tombak I N 1971 *Zh. Prikl. Spektrosk.* **14** 1027 (in Russian)
- [16] Nikl M, Mihoková E and Nitsch K 1992 *Solid State Commun.* **84** 1089
- [17] Murk V, Namosov B and Yarosevich N 1995 *Radiat. Meas.* **24** 371
- [18] Belsky A N, Mikhailin V V, Vasil'ev A N, Dafinei I, Lecoq P, Pedrini C, Chevallier P, Dhez P and Martin P 1995 *Chem. Phys. Lett.* **243** 552